GRAPHENE

Even-denominator fractional quantum Hall states in bilayer graphene

J. I. A. Li,[1*] C. Tan,[2,3] S. Chen,[4] Y. Zeng,[1] T. Taniguchi,[5] K. Watanabe,[5] J. Hone,[2] C. R. Dean[1*]

The distinct Landau level spectrum of bilayer graphene (BLG) is predicted to support a non-abelian even-denominator fractional quantum Hall (FQH) state similar to the $^5/_2$ state first identified in GaAs. However, the nature of this state has remained difficult to characterize. Here, we report transport measurements of a robust sequence of even-denominator FQH in dual-gated BLG devices. Parallel field measurement confirms the spin-polarized nature of the ground state, which is consistent with the Pfaffian/anti-Pfaffian description. The sensitivity of the even-denominator states to both filling fraction and transverse displacement field provides new opportunities for tunability. Our results suggest that BLG is a platform in which topological ground states with possible non-abelian excitations can be manipulated and controlled.

The even-denominator fractional quantum Hall (FQH) state at $^5/_2$ filling in the $N = 1$ Landau level (LL) of GaAs (*1*, *2*) is an intensely studied anomaly in condensed matter physics. Numerical calculations suggest the likely ground state to be the Moore-Read (MR) Pfaffian (*3*–*5*) or its particle-hole conjugate, anti-Pfaffian (*6*–*8*), both of which may be understood as a type of p-wave superconductor resulting from the condensation of composite Fermion pairs. However, despite nearly three decades of experimental effort, a definitive proof remains missing. One of the most intriguing consequences of the Pfaffian description is the expectation that this system naturally hosts Majorana excitations that obey non-abelian fractional statistics (*4*, *9*, *10*). Owing to their theoretical potential to enable topological quantum computation, there has been substantial effort in recent years to engineer systems in which Majorana bound states may be realized (*10*–*13*).

The ground state at half filling is sensitive to the details of the Coulomb interaction, and in GaAs, the $N = 1$ LL proved to be optimal for stabilizing the Pfaffian state (*14*). Experimental studies indicate that the $^5/_2$ state is spin polarized and carries $^e/_4$ fractional charge (*15*), observations that are both consistent with the Pfaffian description. However, demonstrating the predicted non-abelian statistics remains an open challenge (*16*). The fragile nature and limited tunability of the even-denominator state in conventional semiconductor heterostructures have hindered experimental progress (*16*–*18*), motivating the search for a more favorable system that hosts the Pfaffian.

In bilayer graphene (BLG), the $N = 1$ LL has an unusual composition, comprising a mixture of the conventional Landau orbital 0 and 1 wave functions (*19*, *20*), and moreover is accidentally degenerate with the $N = 0$ LL (Fig. 1A) (*21*). Because of this composition, the application of a strong magnetic field, B, can both lift the level degeneracy and modify the precise structure of the $N = 1$ wave function by modifying the relative weight of the conventional 0, 1 contributions. Both of these effects determine the stability of the Pfaffian ground state (*19*, *22*). Additionally, applying a transverse electric field, D, breaks the inversion symmetry between the two sets of graphene lattices and induces phase transitions between ground states with different valley and orbital polarizations (*20*, *23*, *24*). The application of both B and D fields therefore makes it theoretically possible to dynamically tune several key parameters within a single device, including the orbital wave function, effective Coulomb interaction, and LL mixing. Optimizing these parameters in BLG is predicted to yield a more robust even-denominator state than that in GaAs. Tantalizing evidence of an even-denominator state was reported in suspended BLG with a single gate electrode (*25*); however, the suspended geometry limited the ability to identify the associated spin, valley, and orbital order, all distinguishing characteristics of the Pfaffian and anti-Pfaffian states. It was recently reported with a capacitance setup that a ground state with a robust energy gap appears at half filling in the lowest LL (LLL) of BLG (*26*). Numerical computation suggests such ground state to be the Pfaffian.

Here, we report magneto-transport of a sequence of fully developed even-denominator FQH states in ultrahigh mobility BN-encapsulated BLG. Using a dual-gate geometry (Fig. 1B) to tune through different orbital and layer polarizations, we found four even-denominator states appearing within the $N = 1$ orbital branches of the lowest LL, which is consistent with theoretical expectations for either the MR Pfaffian or anti-Pfaffian state in BLG (*19*, *22*, *27*).

The longitudinal conductance σ_{xx} of the LLL as a function of the filling fraction and magnetic field is shown in Fig. 1C. The data in this plot were acquired at fixed displacement field (*28*). The high device quality is evident by the ability to resolve all of the broken-symmetry integer quantum-Hall states, as well as the numerous FQH states observed throughout the phase space (*20*, *24*, *26*). Most notable is the appearance of conductance minima, suggestive of several even-denominator states, occurring at filling fractions $-^5/_2$, $-^1/_2$, $^3/_2$, and $^7/_2$. On the basis of recent understanding of how the eightfold degeneracy of the LLL is lifted at high field (*20*, *29*), we identified that these states appear only at half filling of the broken-symmetry states (BSSs) with orbital index $N = 1$. By contrast, no even-denominator states appear within the $N = 0$ BSSs (*30*–*32*).

Shown in Fig. 1, D and E, are plots of the longitudinal resistance and transverse conductance around $^1/_2$, and $^3/_2$ filling, acquired at fixed density n, and D, while varying B. For $0 \le \nu \le 1$ (Fig. 1D), the wave function is characterized by orbital index $N = 0$ (*20*). A well-developed series of FQH states is observed, following the usual Jain sequence of composite fermions (CFs) (*33*, *34*), with the highest resolvable CF state at $\nu = {}^4/_9$. At half filling, the longitudinal and Hall response both appear featureless. Qualitatively, this sequence closely resembles the FQH hierarchy observed in the $N = 0$ LLs in GaAs (*1*). In stark contrast is the behavior between $1 \le \nu \le 2$, corresponding to a BSS with orbital index $N = 1$ (Fig. 1E). Fewer FQH states are resolved, with $^n/_3$ being the only CF states that appear fully developed. A robust incompressible state is clearly present at $\nu = {}^3/_2$, marked by zero longitudinal resistance simultaneous with a quantized Hall plateau. The qualitative similarity to the $N = 1$ states observed in GaAs (*1*, *2*) and more recently in ZnO (*35*)—both in terms of the even-denominator state appearing at half filling, and its strength relative to the FQH states away from half filling—highlights the important role played by the orbital wave function in determining the interaction-driven behavior.

In order to fully characterize the even-denominator states, we examined the energy gap with variable-temperature activation measurements. Among the four even-denominator states, the size of the energy gap demonstrates an unexpected hierarchy (Fig. 2A), where Δ becomes smaller approaching the edge of the LLL ($\Delta_{-1/2}$ is the largest and $\Delta_{7/2}$ the smallest). Several effects may contribute to this observation, including variation in level mixing, electron interaction strength, and disorder, all of which may be filling fraction–dependent within the LLL.

We focused on the B field dependence of the $\nu = {}^3/_2$ state in order to identify the ground-state

[1]Department of Physics, Columbia University, New York, NY, USA. [2]Department of Mechanical Engineering, Columbia University, New York, NY, USA. [3]Department of Electrical Engineering, Columbia University, New York, NY, USA. [4]Department of Applied Physics and Applied Mathematics, Columbia University, New York, NY, USA. [5]National Institute for Materials Science, 1-1 Namiki, Tsukuba, Japan.
*Corresponding author. Email: jiali2015@gmail.com (J.I.A.L.); cory.dean@gmail.com (C.R.D.)

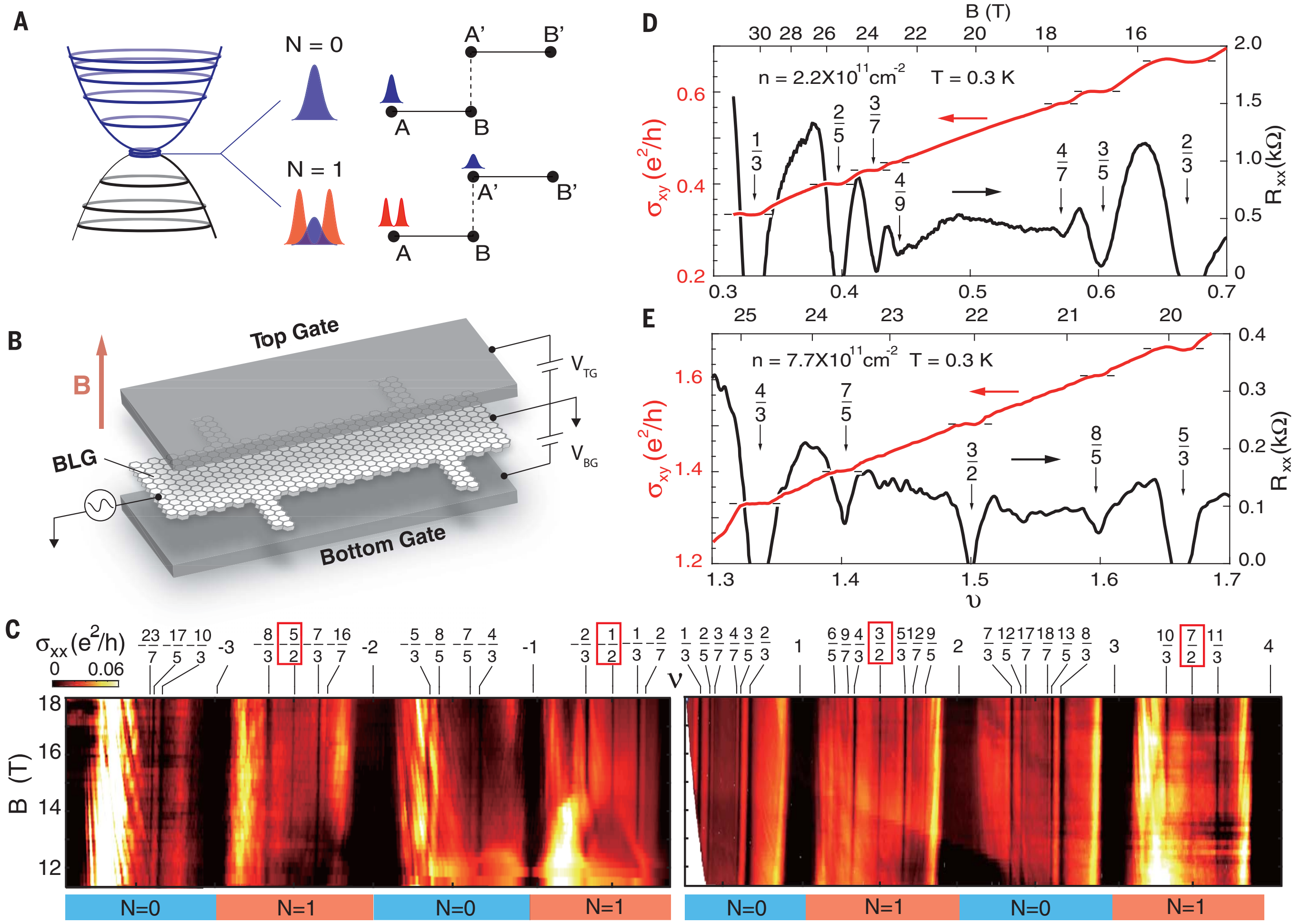

Fig. 1. FQH states in BLG. (**A**) Energy spectrum of the BLG LLs near the charge neutrality point (CNP). The lowest two LLs with Landau orbital index N = 0 and 1 are energetically degenerate, leading to the eightfold degeneracy of the LLL. The BLG wave function with Landau orbital N = 0 is identical to the lowest Landau orbital wave function for conventional (nonrelativistic) systems, whereas the orbital N = 1 wave function is a mixture of the conventional Landau orbitals 0 and 1. The schematic shows the wave function distribution on the four atomic sites of BLG, for the N = 0 and 1 Landau orbital states. The blue-shaded schematic wave function corresponds to conventional Landau orbital 0, and the red-shaded schematic wave function corresponds to conventional Landau orbital 1. (**B**) Schematic of the device geometry. (**C**) σ_{xx} as a function of filling factor ν and magnetic field B at T = 20 mK and (left) D = –100 mV/nm and (right) D = 35 mV/nm for the LLL ($-4 \le \nu \le 4$). (**D** and **E**) σ_{xy} and R_{xx}, acquired by sweeping B at T = 0.3 K and fixed carrier densities, n = 2.2 × 10^{11} cm^{-2} and 7.7 × 10^{11}cm^{-2}, corresponding to filling fractions spanning (D) $0 \le \nu \le 1$ and (E) $1 \le \nu \le 2$. Bottom axis labels the filling fraction ν, with corresponding B values on the top axis.

wave function and examine its tunability. The measured gap shows a nonmonotonic behavior (Fig. 2B), increasing to ~3.5 K at 25 T before then diminishing under higher fields. This behavior is not explained by the usual interaction-driven picture in which the gap scales with the Coulomb energy, $E_c = \frac{e^2}{\varepsilon \ell_B}$. Here, e is the electron charge, ε is the dielectric constant, and $\ell_B \approx 26\,\text{nm}/\sqrt{B}$ is the magnetic length. However, this is consistent with previous theoretical considerations of BLG in which beyond a critical magnetic field, a transition from a gapped incompressible state to a gapless composite Fermi liquid state is expected (*19*, *22*). This is a consequence of an increasing orbital 0 component in the N = 1 wave function with increasing field. This interpretation is qualitatively consistent with the B field evolution of the overall structure of the LL (Fig. 2C) in which, around magnetic fields similar to where the gap maximum occurs, we see the development of a complete sequence of Jain FQHE states, which is indicative of a growing orbital 0 component, with well-resolved features developing at $1 + {}^2/_5$, $1 + {}^3/_7$, and their respective conjugates. The particle-hole symmetry between the $1 + {}^2/_5$ and $1 + {}^3/_5$ states is evidence that these two states originate from the orbital 0 component, which is different from the exotic $2 + {}^2/_5$ state reported in the GaAs quantum well (*36*, *37*).

Next, we probed the spin order of the ground state by applying a parallel magnetic field ($B_\parallel$) while keeping the perpendicular field ($B_\perp$) fixed (Fig. 2D). The energy gap values show no parallel field dependence up to the largest applied value of $B_\parallel$ ~ 25 T. This indicates a spin-polarized ground state, consistent with the Pfaffian/anti-Pfaffian, and rules out possible spin-singlet candidate wave functions that may give rise to an even-denominator state, such as the Halperin (331) (*38*). Our result moreover supports the long-held theoretical conjecture that the decrease with $B_\parallel$ of the gap of the ${}^5/_2$ state in GaAs (*39*) is caused by transverse orbital effects owing to the finite quantum well width (*3*, *40*). In our BLG device, by contrast, the crystal is less than 1 nm thick and therefore insensitive to these effects within accessible field ranges. Taken together, our results provide compelling evidence that in the absence of some other, as yet unidentified ground state, the even-denominator FQH states observed here likely correspond to the MR Pfaffian, or its particle-hole conjugate (*6*, *7*).

BLG is tunable under a perpendicular electric field D. We plotted in Fig. 3A σ_{xx} versus D and ν

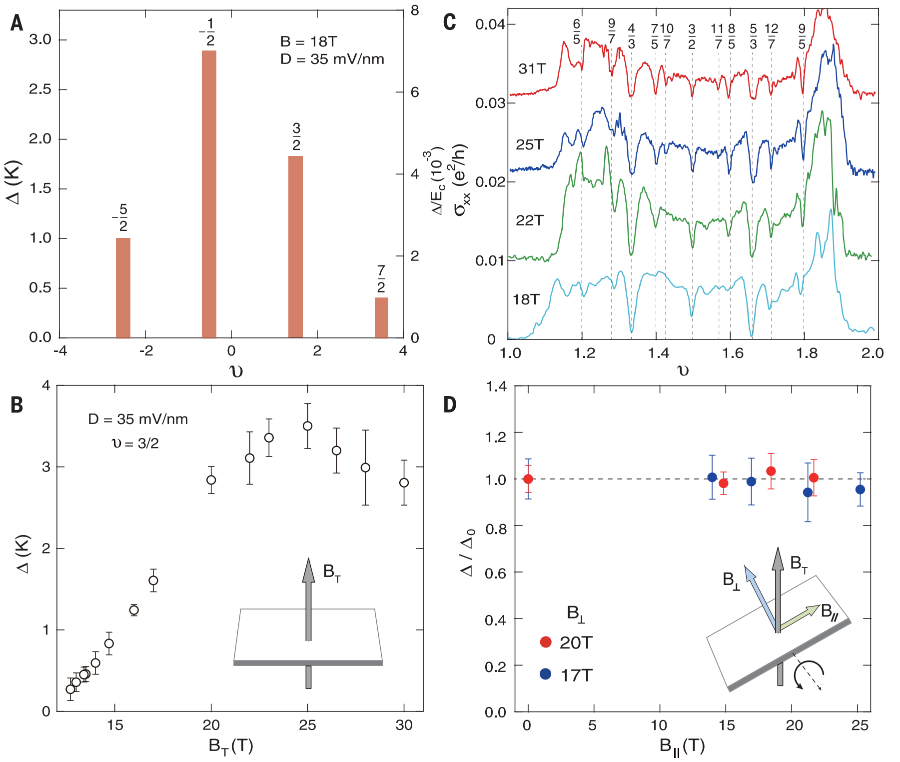

Fig. 2. Behavior of the energy gap. (**A**) Δ for all even-denominator states at B = 18 T and D = 35 mV/nm. (**B**) Δ of the $v = {}^{3}/_{2}$ state as a function of magnetic field B, at D = 35 mV/nm and T = 0.3 K. (**C**) Longitudinal conductance σ_{xx} versus v at different B. Measurements are performed by changing carrier density n while keeping displacement field constant at D = 35 mV/nm. Traces are offset for clarity. (**D**) Energy gap of the $v = {}^{3}/_{2}$ state normalized to its $B_{\parallel}$ = 0 value, versus parallel field for two fixed values of perpendicular field.

for $0 \leq v \leq 4$, the electron half of the LLL (similar analysis of the valence band states is shown in fig. S4). A schematic phase diagram of the orbital and valley ordering associated with each state is shown in Fig. 3B. We labeled the orbital and valley orderings $|\zeta N\rangle$ based on recent capacitance spectroscopic measurement of BLG (*20*, *26*), where $\zeta = K, K'$ is the valley isospin and N = 0 and 1 is the Landau orbital.

Qualitatively, we found that even-denominator states are insensitive to the changes in the valley ordering, persisting smoothly across D-induced transition boundaries. For example, the ${}^{7}/_{2}$ state is well developed over both the K' (D > 0) and K (D < 0) regions. Likewise, the ${}^{3}/_{2}$ state remains stable through four different valley orderings as D is varied. The ${}^{3}/_{2}$ state disappears near D = 0, but this corresponds to a transition to a N = 0 orbital, which is consistent with the same selection rule identified above. That the even-denominator state is sensitive to orbital structure but insensitive to valley order is consistent with theoretical treatment of the Pfaffian in BLG (*19*, *22*). However, it is curious that the state remains stable near the transition boundary, where the effects of LL mixing are expected to be most prominent (*8*, *41*) and typically assumed to play a destructive role. No FQH state appears to form at ${}^{1}/_{2}$ and ${}^{5}/_{2}$ filling, even within regions where a D-induced orbital transition to N = 1 is realized.

The effect of the displacement field on the variation of Δ is shown in Fig. 3C. For all of the even-denominator states, the gap is observed to decrease continuously with increasing D, with no apparent correlation to the valley-ordering

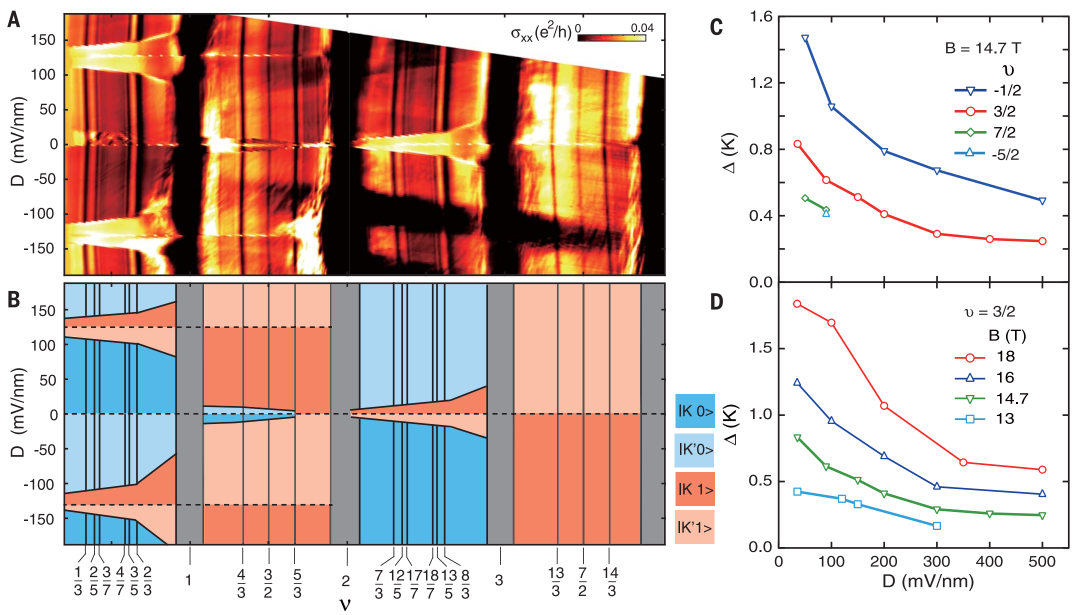

Fig. 3. Tuning with displacement field. (**A**) σ_{xx} at T = 0.2 K and B = 14.7 T versus filling factor v and displacement field D for the LLL of BLG, $0 \leq v \leq 4$. (**B**) Schematic phase diagram labeling the ground-state order for the same filling fraction range as shown in (A). The blue- and red-shaded areas are occupied by broken-symmetry states with orbital index 0 and 1, respectively, whereas the dark and light color tones denote respectively the two different valley-isospin and layer polarizations. Dashed and solid black lines correspond to phase transitions between broken-symmetry states with different valley-isospin and orbital index, respectively. Vertical solid lines represent incompressible states observed in transport measurements. (**C**) Δ as a function of D for $v = -{}^{1}/_{2}, {}^{3}/_{2}, -{}^{5}/_{2}$, and ${}^{7}/_{2}$ at B = 14.7 T. (**D**) Δ versus D for $v = {}^{3}/_{2}$ at various B.

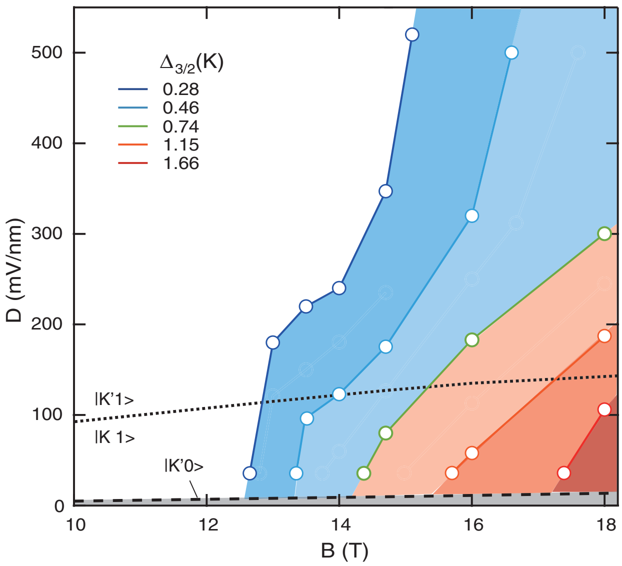

Fig. 4. Phase diagram for the 3/2 state gap. Shown is the contour line for $\Delta_{3/2}$ as a function of B and D. The valley polarization transition at nonzero D is shown as the black dotted line, and the orbital polarization transition is shown as the black dashed line. The even-denominator state disappears in the orbital 0 region (gray-shaded area).

phase diagram. The D-induced gap variation is larger than theoretical predictions (*19*), and the origin of this surprising result is not known. D dependence appears to vary with B (Fig. 3D). This behavior is summarized in the experimentally measured B – D phase diagram for the $^{3}/_{2}$ state gap, shown in Fig. 4. Also shown in this diagram are the D field values for the valley (Fig. 4, black dotted line) and orbital (Fig. 4, black dashed line) transitions. Within our data resolution, there is no discernible dependence on the valley order. In Fig. 4, $\Delta_{3/2}$ is too small to measure in the white area and is absent altogether in the gray shaded area, where the ground state wave function has orbital index N = 0. Although we rule out a spin-singlet ground state origin for the even-denominator state, a valley singlet equivalent (331) state could be possible. However, we consider this unlikely because we observed the gap to persist to large displacement fields, where the system is presumed to be fully layer-polarized (*20*, *23*, *24*, *29*).

Our observations demonstrate that within the LLL of BLG, the gap of the even-denominator state can be sensitively tuned by varying density, B, and D. The unexpected coupling to the D field suggests that there is much we do not understand about the nature of even-denominator states in BLG. Just as the Pfaffian ground state is expected to be replaced by the composite fermion liquid with increasing B (*19*, *22*), the D dependence of the energy gap could be indicative of a phase transition to a different ground state.

The observation of a robust and dynamically tunable even-denominator FQH state in BLG provides a rich platform in which to probe the nature of an exotic ground state. The ability to reach a regime where the transport gap exceeds 3 K together with the ability to tune the stability of the gap makes the state accessible to a wider range of experimental probes than previously possible in GaAs. Moreover, the use of thin hexagonal boron nitride (hBN) dielectrics combined with the two-dimensional nature of the BLG crystal may enable the electrostatic control necessary to investigate the presumed non-abelian statistics through new interferometry experiments (*18*).

REFERENCES AND NOTES

1. R. Willett *et al.*, *Phys. Rev. Lett.* **59**, 1776–1779 (1987).
2. W. Pan *et al.*, *Phys. Rev. Lett.* **83**, 3530–3533 (1999).
3. R. H. Morf, *Phys. Rev. Lett.* **80**, 1505–1508 (1998).
4. G. Moore, N. Read, *Nucl. Phys. B* **360**, 362 (1991).
5. M. Greiter, X.-G. Wen, F. Wilczek, *Phys. Rev. Lett.* **66**, 3205–3208 (1991).
6. M. Levin, B. I. Halperin, B. Rosenow, *Phys. Rev. Lett.* **99**, 236806 (2007).
7. S.-S. Lee, S. Ryu, C. Nayak, M. P. A. Fisher, *Phys. Rev. Lett.* **99**, 236807 (2007).
8. E. H. Rezayi, *Phys. Rev. Lett.* **119**, 026801 (2017).
9. N. Read, E. Rezayi, *Phys. Rev. B Condens. Matter* **54**, 16864–16887 (1996).
10. C. Nayak, S. H. Simon, A. Stern, M. Freedman, S. Das Sarma, *Rev. Mod. Phys.* **80**, 1083–1159 (2008).
11. A. Kitaev, *Ann. Phys.* **303**, 2–30 (2003).
12. L. Fu, C. L. Kane, *Phys. Rev. Lett.* **100**, 096407 (2008).
13. V. Mourik *et al.*, *Science* **336**, 1003–1007 (2012).
14. E. H. Rezayi, F. D. M. Haldane, *Phys. Rev. Lett.* **84**, 4685–4688 (2000).
15. R. L. Willett, *Rep. Prog. Phys.* **76**, 076501 (2013).
16. B. I. Halperin, A. Stern, I. Neder, B. Rosenow, *Phys. Rev. B* **83**, 155440 (2011).
17. R. L. Willett, L. N. Pfeiffer, K. W. West, *Proc. Natl. Acad. Sci. U.S.A.* **106**, 8853–8858 (2009).
18. W. Bishara, C. Nayak, *Phys. Rev. B* **77**, 165302 (2008).
19. V. M. Apalkov, T. Chakraborty, *Phys. Rev. Lett.* **107**, 186803 (2011).
20. B. M. Hunt *et al.*, *Nat. Commun.* **8**, 948 (2017).
21. E. McCann, V. I. Fal'ko, *Phys. Rev. Lett.* **96**, 086805 (2006).
22. Z. Papić, D. A. Abanin, Y. Barlas, R. N. Bhatt, *Phys. Rev. B* **84**, 241306 (2011).
23. R. T. Weitz, M. T. Allen, B. E. Feldman, J. Martin, A. Yacoby, *Science* **330**, 812–816 (2010).
24. P. Maher *et al.*, *Science* **345**, 61–64 (2014).
25. D.-K. Ki, V. I. Fal'ko, D. A. Abanin, A. F. Morpurgo, *Nano Lett.* **14**, 2135–2139 (2014).
26. A. A. Zibrov *et al.*, *Nature* **549**, 360–364 (2017).
27. Z. Papić, D. A. Abanin, *Phys. Rev. Lett.* **112**, 046602 (2014).
28. Materials and methods are available as supplementary materials.
29. A. Kou *et al.*, *Science* **345**, 55–57 (2014).
30. Y. J. Song *et al.*, *Nature* **467**, 185–189 (2010).
31. Y. Kim *et al.*, *Nano Lett.* **15**, 7445–7451 (2015).
32. Y.-H. Wu, T. Shi, J. K. Jain, *Nano Lett.* **17**, 4643–4647 (2017).
33. J. K. Jain, *Phys. Rev. Lett.* **63**, 199–202 (1989).
34. J. K. Jain, *Composite Fermions* (Cambridge Univ. Press, 2003).
35. J. Falson *et al.*, *Nat. Phys.* **11**, 347–351 (2015).
36. A. Kumar, G. A. Csáthy, M. J. Manfra, L. N. Pfeiffer, K. W. West, *Phys. Rev. Lett.* **105**, 246808 (2010).
37. K. Pakrouski, M. Troyer, Y.-L. Wu, S. Das Sarma, M. R. Peterson, *Phys. Rev. B* **94**, 075108 (2016).
38. F. D. M. Haldane, *Phys. Rev. Lett.* **51**, 605–608 (1983).
39. J. P. Eisenstein *et al.*, *Phys. Rev. Lett.* **61**, 997–1000 (1988).
40. M. R. Peterson, T. Jolicoeur, S. Das Sarma, *Phys. Rev. B* **78**, 155308 (2008).
41. E. H. Rezayi, S. H. Simon, *Phys. Rev. Lett.* **106**, 116801 (2011).

ACKNOWLEDGMENTS

The authors thank Z. Papic, A. Young, and X. Liu for helpful discussion. This work was supported by the National Science Foundation (grant DMR-1507788). C.R.D acknowledges partial support by the David and Lucile Packard Foundation. C.T. is supported by INDEX. A portion of this work was performed at the National High Magnetic Field Laboratory, which is supported by National Science Foundation Cooperative Agreement DMR-1157490 and the State of Florida.

SUPPLEMENTARY MATERIALS

www.sciencemag.org/content/358/6363/648/suppl/DC1
Materials and Methods
Figs. S1 to S10
Reference (*42*)

30 June 2017; accepted 25 September 2017
Published online 5 October 2017
10.1126/science.aao2521

Science

Even-denominator fractional quantum Hall states in bilayer graphene

J. I. A. Li, C. Tan, S. Chen, Y. Zeng, T. Taniguchi, K. Watanabe, J. Hone and C. R. Dean

Science **358** (6363), 648-652.
DOI: 10.1126/science.aao2521originally published online October 5, 2017

Exotic states pop up in bilayer graphene
Particles with exotic quantum statistics are expected to be able to support an especially appealing flavor of quantum computing (QC) called topological QC. A particular fractional quantum Hall state in the semiconductor GaAs has long been thought to possess excitations with these favorable properties, but proving so has turned out to be tricky. Working with bilayer graphene instead of GaAs, Li *et al.* found four states that appear to be consistent with the theoretical description of states with the required quantum statistics. The researchers were able to tune the properties of these states by applying an electric field, adding a valuable control knob.
Science, this issue p. 648

Science (print ISSN 0036-8075; online ISSN 1095-9203) is published by the American Association for the Advancement of Science, 1200 New York Avenue NW, Washington, DC 20005. The title *Science* is a registered trademark of AAAS.